JOURNAL OF MATERIALS SCIENCE 25 (1990) 563–566

Electron microscopic study on the oxidation of β-tin irradiated by electron beam

KOZO OJIMA, YOUJI TANEDA
Department of Mathematics and Physics, The National Defence Academy, Hashirimizu, Yokosuka 239, Japan

Effects of electron beam irradiation to β-tin thin foils have been studied using high-resolution electron microscopy. By the beam irradiation, the β-tin crystal at the extreme-thin foil region disappear, and amorphous oxide films covering the β-tin crystal are converted into SnO_2 micro-crystallites of about 5 to 10 nm in diameter. The present study also shows that the causes for the development of SnO_2 are not due to the increment in the temperature of amorphous and β-tin regions resulting from the electron irradiation. It seems that the conversion into SnO_2 is caused by the ionization action of electron beam to atom species.

1. Introduction

Studies of oxidation of β-tin are of technological interest for problems associated with the preparation of transparent conduction thin films of SnO_2 as well as the theoretical or physical interest of the oxidation process. Several studies have been reported on the oxidation of β-tin. Bevolo, Verhoeven and Noack [1] have investigated the oxidation of metallic tin by oxygen exposure using low energy electron loss spectroscopy and Auger spectroscopy. They showed in the investigation that from zero to one monolayer the oxide grew as islands containing both SnO and SnO_2. Sen *et al.* [2] have concluded from both Auger electron spectroscopy and transmission electron microscopy that tin foils exposed to dry oxygen of 100 KPa are oxidized to SnO on annealing for up to 12 h at 200° C, but longer annealing produces further oxidation to SnO_2. On the other hand, Damodare Das [3] has reported that selected-area electron diffraction patterns of β-tin films deposited in vacuum of 2×10^{-3} Pa – 1×10^{-1} Pa do not reveal any presence of oxides in the film.

The conversion of vacuum-deposited β-tin films irradiated by the electron beam into SnO_2 has been confirmed using electron diffraction technique by Eyring and Dufner [4]. However, no studies using high resolution electron microscopy (HREM) have been made to investigate the oxidation of β-tin, although excellent studies on atomic imaging of oxide surfaces in various materials have been recently reported by Smith *et al.* [5–7].

In the present work, oxidations of β-tin foils irradiated by the electron beam are investigated in detail using HREM and electron diffraction technique. The direct observations at the atomic level clearly show the conversion of β-tin crystals into SnO_2 micro-crystallites.

2. Experimental procedure

β-tin used in this study was obtained from Mitsubishi Metal Company in the form of ingot, having a purity of 99.999%. Controlled orientation single crystals, with the growth axis in the [1 1 0] direction and the top surface parallel to the (0 0 1) planes, were grown from the melt in a modified Bridgman furnace, under a vacuum of 2×10^{-4} Pa. The single crystals grown in slabs of rectangular cross-section of 1 mm × 6 mm were a thinned down form of HREM observation by chemical and subsequent electrolytic polishing. The methods have been described in detail elsewhere [8]. The polish was followed by a rapid and thorough water rinse, and then by an alcohol rinse.

To examine the electron microscope image of oxide resulting from heating, some of the produced thin foils were heat treated at 100° C and 200° C for 1–6 h in a furnace under a vacuum of 2×10^{-4} Pa.

The β-tin thin foils were irradiated for about a 6 h period by electron beam in a JEOL 200-CX electron microscope operating at 200 kV, equipped with a top-entry-type goniometer stage and a LaB_6 filament. The beam current densities were about in 50 A cm^{-2}. The vacuum in the electron microscope is the order of 10^{-4} Pa which is the same order as that in the heat treating furnace. The spherical aberration coefficient of the objective lens was 1.2 mm. In this study, for a set of through-focal series of images, five micrographs were taken in every 45 nm increments of focus, starting at the minimum–contrast condition. Each of the series was photographed at about 10 min intervals until an hour period and at about once every half hour after the period. Images were usually recorded at a magnification of 360 000 times. Care was taken to align the foil under axial illumination conditions – to avoid the spurious Fourier images. The lattice imaging was achieved by use of 37 diffraction waves.

3. Results and discussion

A series of wide-field views of HREM images typically showing the effects of electron beam irradiation to β-tin thin foils and the corresponding selected-area

0022–2461/90 $03.00 + .12

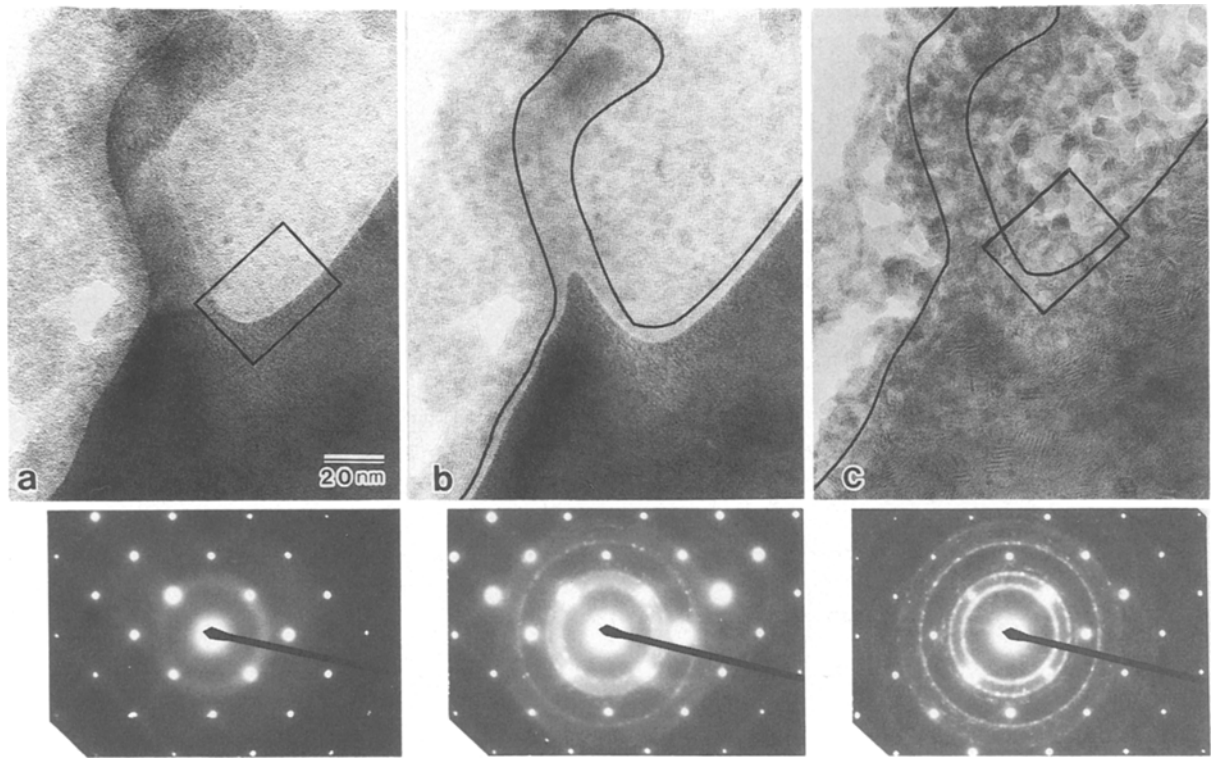

Figure 1 A series of electron micrographs showing the effects of electron beam irradiation and the corresponding selected-area diffraction patterns, (a) soon after the initial irradiation, (b) after a beam irradiation of 20 min, (c) after a beam irradiation of 6 h. Diffraction rings are from SnO_2 micro-crystallites.

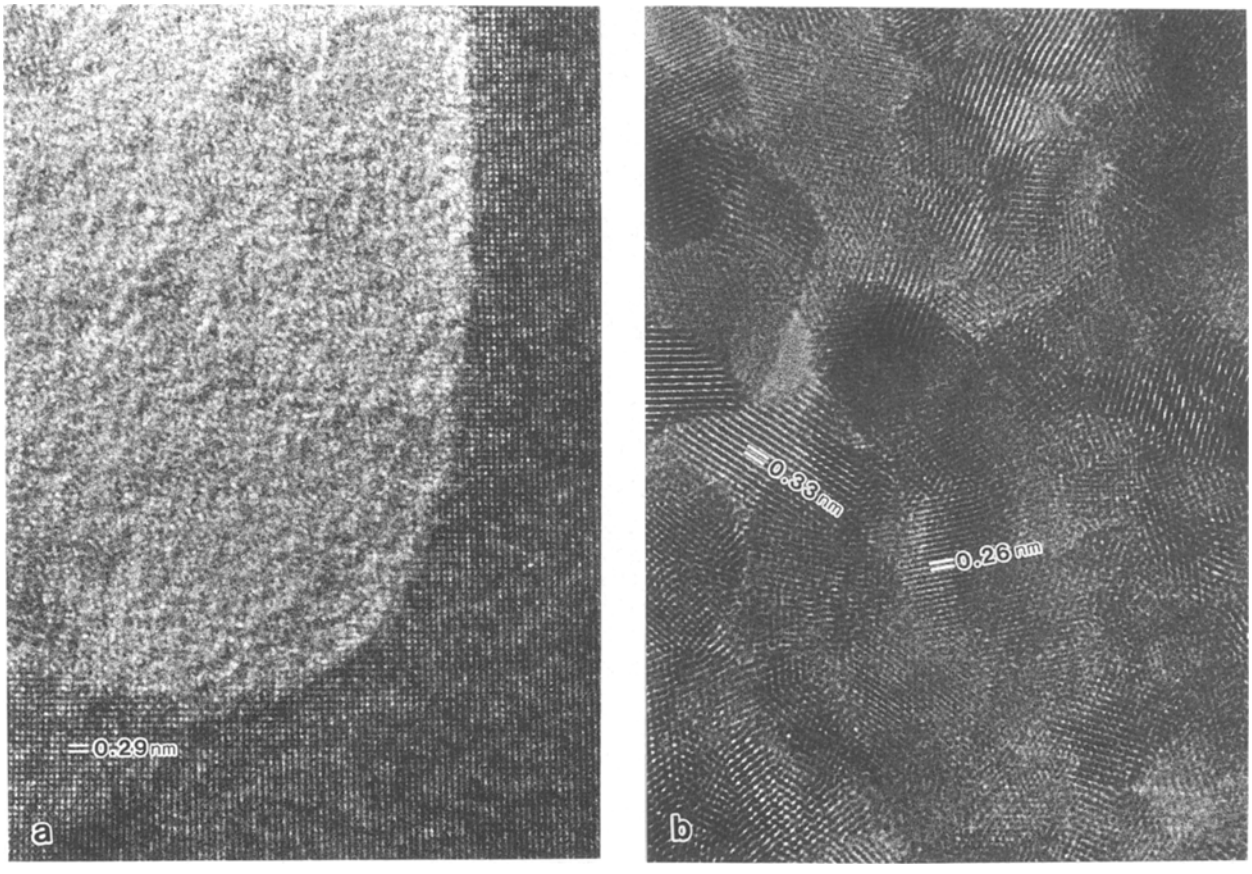

Figure 2 (a) The photographically enlarged micrograph of the boxed region in Fig. 1(a). (b) The photographically enlarged micrograph of the boxed region in Fig. 1(c). (b) The appearance after beam irradiation of 6 h at the same region as (a).

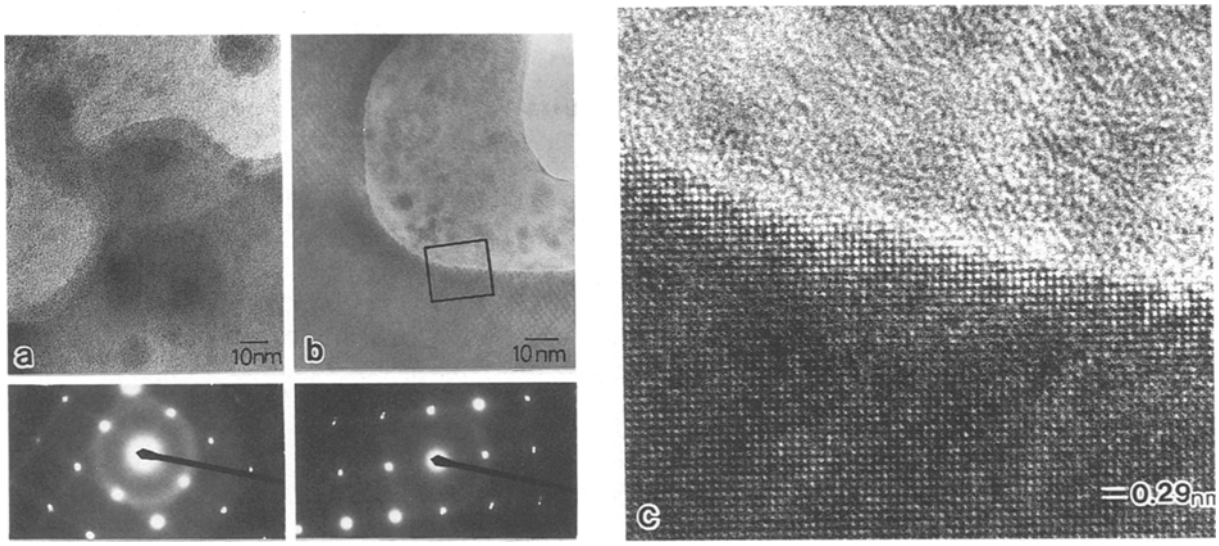

Figure 3 Heat treated β-tin thin foils: (a) at 100° C for 6 h, (b) at 200° C for 6 h, (c) enlarged micrograph of boxed region in (b). No developments of SnO_2 crystallites are observed in both of the figures.

electron diffraction patterns are shown in Figs 1(a)–(c). Figure 1(a) shows the appearance of a foil photographed almost soon after it was irradiated to the 200 kV electron beam. Figures 1(b) and (c) show the micrographs after irradiation of 20 min and 6 h to electron beam respectively. The dark-coloured regions of Figs 1(a) and (b) correspond to the region of β-tin crystal, which was confirmed by the lattice fringe in the HREM image. A curve in Fig. 1(b) delineates the edge of the β-tin crystal in Fig. 1(a). Shrinkage of the β-tin crystal region is clearly found from comparing these figures. It is deduced that the temperature at the β-tin regions was not raised above 157° C during microscopy session since indium thin foil did not melt in the same way with this electron beam irradiation experiment. So the shrinkage is not due to the evaporation of β-tin crystal.

In general, a thin film of about 100–300 nm in width along the edge of the region of β-tin crystal, as shown by the bright-coloured region in Fig. 1(a), is observed soon after initial irradiation to the electron beam. It is evident that the materials in the large part of the film of amorphous since they give diffuse rings in the electron diffraction patterns (see Fig. 1(a)), and the HREM images of the films show the speckled structure that is characteristic of amorphous materials, as shown later in Fig. 2(a). The amorphous materials are supposed to be the oxide thin films resulting from the electrolytic polishing or oxidation in air after the treatment – the β-tin thin foil is covered with the layers of the oxide thin films.

The electron diffraction patterns in Figs 1(b) and (c) show the rings from SnO_2 crystallines together with the spots from a (0 0 1) β-tin single crystal. The ring patterns in Figs 1(a)–(c) disclose the presence of SnO_2 crystallites which is marked by the increasing diffraction intensity of SnO_2 with increasing period of electron irradiation. The change of the diffraction patterns implies that the region of β-tin shown in Fig. 1 experienced oxidation in the electron beam during the microscopy session. The region indicated by the box in Fig. 1(a) is the same as the boxed region in Fig. 1(c). The boxed regions in Figs 1(a) and (c) are photographically enlarged in Figs. 2(a) and (b), respectively, to show details of lattice image.

The availability of HREM enables the detailed information about structural morphology of the crystals. The β-tin and amorphous shown in Fig. 2(a) have been converted into the micro-crystallites shown in Fig. 2(b) after 6 h in the electron beam. The crystallites are further confirmed as SnO_2 crystals by careful cross calibration of lattice fringe spacings of HREM images. Examples are indicated in Fig. 2(b) as SnO_2 (1 1 0) fringes of 0.33 nm and (1 0 1) fringes of 0.26 nm. The SnO_2 micro-crystallites had diameters of about 5–10 nm. The conversion into SnO_2 crystallites has been initially observed after about 10 min in the beam, and the size and orientation of the crystallites changed gradually with the lapse of time. As shown in Fig. 2(b), further exposure led eventually to the overlap of their crystallites. The overlapping shows the grain growth of SnO_2 particles, although it was impossible in this experiment to make clear the morphology of the growth at atomic level.

Moiré fringes appeared in the region of β-tin crystal after about 30 min in the beam. The appearance of moiré fringes, as shown in Fig. 1(c), denotes that the oxide amorphous layers covered the β-tin crystal has converted into the SnO_2 micro-crystallites. Furthermore, it is deduced from the result of the shrinkage of β-tin crystal that the oxidation of β-tin into SnO_2 is developed by the interdiffusions between tin and oxygen atoms supported by successive electron beam irradiation.

Representative results of the heating experiments are shown in Fig. 3. Figures 3(a) and (b) denote the effects of heating at 100° C for 6 h and at 200° C for 6 h, respectively. In these figures, also shown are the selected-area diffraction patterns from the regions imaged. These were photographed soon after electron beam irradiation. The regions of β-tin crystals correspond to the dark-coloured region in Figs 3(a) and (b).

No developments of SnO_2 crystallites in the heat treated β-tin thin foils are recognized as indicated by diffraction rings in Figs 3(a) and (b). Figure 3(c) shows the enlarged micrograph of the boxed region in Fig. 3(b). SnO_2 crystallites in the amorphous regions of heat treated foils are scarcely observed, and further, no moiré fringes are observed in the β-tin crystal regions, as shown in Fig. 3(c).

The number of developments of SnO_2 crystallites in the heat treated β-tin thin foils are recognized as indicated by diffraction rings in Figs 3(a) and (b). Figure 3(c) shows the enlarged micrographs of boxed region in Fig. 3(b). SnO_2 crystallites in the amorphous regions of heat treated foils are scarcely observed, and further, no moiré fringes are observed in the β-tin crystal regions, as shown in Fig. 3(c).

It is clear from these results that the development of SnO_2 crystallites during the electron beam irradiation period is not due to the effects of the increment in the temperature of the amorphous and β-tin regions caused by energy absorption from the electron beam. So that, it seems likely that the conversion of β-tin crystals and the amorphous oxide materials into SnO_2 micro-crystallites has been promoted with the reinforcement effect of electron beams to ionization of atom species. Experiments are now in progress to identify the sources of oxygen.

4. Conclusions

The presence of SnO_2 crystallites caused by the electron irradiation to β-tin crystal during microscopy session has been confirmed by HREM observation. The conversion of β-tin into SnO_2 has also been marked by the increasing diffraction intensity of SnO_2 with increasing period of electron irradiation. On the other hand, no developments of SnO_2 crystallites in the heat treated β-tin foils to 100° C or to 200° C were recognized from the HREM observation and selected-area diffraction patterns. So that, the causes for the development of SnO_2 are not due to the increment in the temperature of β-tin regions resulting from the electron irradiation. It seems that the development of SnO_2 crystallites during the electron beam irradiation period is caused by the ionization action of electron beam to atom species.

References

1. A. J. BEVOLO, J. D. VERHOEVEN and M. NOACK, *Surf. Sci.* **134** (1983) 499.
2. S. K. SEN, S. SEN and C. L. BAUER, *Thin Solid Films* **82** (1981) 157.
3. V. DAMODARE DAS, *J. Mater. Sci.* **17** (1982) 2613.
4. L. EYRING and D. C. DUFNER, *Thin Solid Films* **142** (1986) 101.
5. D. J. SMITH, L. A. BURSILL and G. J. WOOD, *J. Solid State Chem.* **50** (1983) 51.
6. D. J. SMITH, L. A. FREEMAN, FRANK J. BERRY and C. HALLETT, *J. Solid State Chem.* **58** (1985) 342.
7. D. J. SMITH, L. A. BURSILL and D. A. JEFFERSON, *Surf. Sci.* **175** (1986) 673.
8. K. OJIMA and Y. TANEDA, *Jpn. J. Appl. Phys.* **27** (1988) L 496.

Received 25 November 1988
and accepted 8 May 1989